The Effect of Wind on the Dispersal of the Hudson River Plume

BYOUNG-JU CHOI* AND JOHN L. WILKIN

Institute of Marine and Coastal Sciences, Rutgers, The State University of New Jersey, New Brunswick, New Jersey

(Manuscript received 10 July 2006, in final form 10 October 2006)

ABSTRACT

The dispersal of the Hudson River plume in response to idealized wind forcing is studied using a three-dimensional model. The model domain includes the Hudson River and its estuary, with a realistic coastline and bottom topography of the New York Bight. Steady low river discharge typical of mean conditions and a high-discharge event representative of the spring freshet are considered. Without wind forcing the plume forms a southward coastally trapped current at low river discharge and a large recirculating bulge of low-salinity water during a high-discharge event. Winds affect the freshwater export through the mouth of the estuary, which is the trajectory the plume takes upon entering the waters of the Mid-Atlantic Bight inner shelf, and the rate at which freshwater drains downstream. The dispersal trajectory is also influenced by the particular geography of the coastline in the apex of the New York Bight. Northward wind causes offshore displacement of a previously formed coastally trapped plume and drives a new plume along the Long Island coast. Southward wind induces a strong coastal jet that efficiently drains freshwater to the south. Eastward wind aids freshwater export from the estuary and favors the accumulation of freshwater in the recirculating bulge outside the mouth of Raritan Bay. Westward wind delays freshwater export from Raritan Bay. The momentum balance of the modeled plume shows that buoyancy and wind forces largely determine the pattern of horizontal freshwater dispersal, including the spreading of freshwater over ambient, more saline water and the bulge formation.

1. Introduction

Observations and numerical simulations have shown that local wind forcing significantly affects the dispersal of a river plume as it enters the coastal ocean (Pullen and Allen 2000; Fong and Geyer 2001; García Berdeal et al. 2002; Janzen and Wong 2002; Whitney and Garvine 2006). This is particularly true of surface-advected plumes where the river outflow forms a thin layer riding on more dense shelf water, and consequently has diminished interaction with the bathymetry (Yankovsky and Chapman 1997). Surface-advected plumes form a freshwater bulge at the mouth of an estuary that can grow without reaching a steady state (Fong and Geyer 2002) until an external forcing agent, such as wind or an ambient along-shelf current, acts to transport freshwater away (Fong and Geyer 2001; Yankovsky et al. 2001; Whitney and Garvine 2005).

Idealized numerical simulations of river plumes are typically formulated with a straight coastline and a river represented by a point source from the wall or a short channel (Chao and Boicourt 1986; Fong and Geyer 2001, 2002; García Berdeal et al. 2002; Hetland 2005), possibly with the addition of time variability in either the river flow (Yankovsky and Chapman 1997) or winds (Hetland 2005). Other plume modeling studies have employed realistic geometry and imposed observed river flow, wind forcing (Pullen and Allen 2000), and tides (Whitney and Garvine 2006) to analyze the dispersal of a particular river plume in comparison with observations. The model presented here is intermediate in realism, and is idealized with respect to variability in wind forcing, river discharge, and initial ocean stratification, but formulated with the coastline, bathymetry, and tidal forcing of the New York Bight into which flows the Hudson River.

This modeling study was conceived as a component of the Lagrangian Transport and Transformation Ex-

* Current affiliation: College of Oceanic and Atmospheric Sciences, Oregon State University, Corvallis, Oregon.

Corresponding author address: Byoung-Ju Choi, College of Oceanic and Atmospheric Sciences, Oregon State University, 104 COAS Admin. Building, Corvallis, OR 97331-5503.
E-mail: bjchoi@coas.oregonstate.edu

DOI: 10.1175/JPO3081.1

© 2007 American Meteorological Society

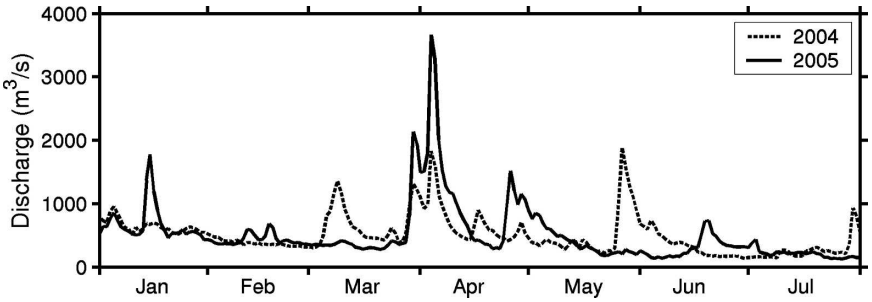

FIG. 1. The Hudson River discharge in 2004 (dotted) and 2005 (solid). The river discharge data were obtained from Hudson River at Fort Edward (USGS stream gauge 01327750) and Mohawk River at Cohoes (USGS stream gauge 01357500). The magnitude of river discharge was multiplied by 1.3 to account for adjacent watershed areas and lateral inflow of tributaries.

periment (LaTTE) (Chant et al. 2006), a multidisciplinary study of the physical, biological, and chemical processes that mix materials in the Hudson River plume and transport them along the coast and across the inner New Jersey shelf. Mean Hudson River flow is 460 $m^3 s^{-1}$, but the discharge stays below this for most of the year, punctuated by high precipitation storm events and the spring freshet when melting snow increases the river discharge, producing one or two significant flow maxima in April and May (Fig. 1). Peak flow values range from 1200 to 3000 $m^3 s^{-1}$, and a high-discharge event generally lasts about 20 days. The river flow becomes partially mixed with ocean water within the river and estuary by tides (Blumberg et al. 1999; Peters 1999; Warner et al. 2005a), discharging as a surface-advected plume. Observations show that the shape and spread of the plume is influenced by local winds (Bowman 1978; Bowman and Iverson 1978; Johnson et al. 2003).

LaTTE field studies were performed during low river discharge conditions (500 $m^3 s^{-1}$) in May 2004 and a high river discharge event (3000 $m^3 s^{-1}$) in April 2005. During these periods surface winds over the New York Bight blew to diverse directions, rather than to any prevailing direction, at mean speeds of around 5 m s^{-1}. In 2005 a large low-salinity bulge formed whereas in 2004 it did not. In both years the trajectory of discharged waters altered in rapid response to variable winds (Hunter et al. 2006), alternately traveling along both the Long Island and New Jersey coasts over the course of the 2004 experiment, but residing within a bulge for a protracted period in 2005. The biogeochemical and ecosystem transformations of interest in LaTTE occur over a matter of days after the estuary discharge reaches the ocean, so the initial plume dispersal process is as important as the subsequent coastal current formation in determining the fate of riverborne material. The coastline geometry of New York Bight is such that winds directed *along* the New Jersey coast blow *across* the Long Island coast, and the bathymetry of the inner shelf is deeply incised by the Hudson shelf valley (Fig. 2). Idealized studies (e.g., Fong and Geyer 2002) that consider straight coasts and uniform bathymetry are therefore incomplete for developing intuition on how the Hudson River plume behaves. A further complication is the narrow estuary mouth between Raritan Bay and the New York Bight. This has similarities with the Delaware Bay where winds within the estuary exert influence on discharge to the shelf (Janzen and Wong 2002; Whitney and Garvine 2005) by temporarily storing water within the bay.

In this paper we use a three-dimensional ocean circulation model to develop insight on how the Hudson River plume responds to winds from varying directions, at varying speeds, during both sustained low-discharge conditions and a high-discharge event. The numerical model setup and initialization are described in the next section. The responses of the plume to wind forcing during low river discharge are presented in section 3. The formation of a large freshwater bulge during a high river discharge event, and changes in its structure resulting from wind forcing, are shown in section 4. Interpretations of the numerical simulations are summarized in section 5.

2. Numerical model and initialization

a. Numerical model setup: Domain, boundary conditions, and forcing

The numerical model used is the Regional Ocean Modeling System (ROMS; information online at http://www.myroms.org), a three-dimensional, free-surface, hydrostatic, split-explicit, primitive-equation ocean model that has been employed in many studies of estuaries, river plumes, and inner-shelf circulation (MacCready and Geyer 2001; Hetland 2005; Warner et al.

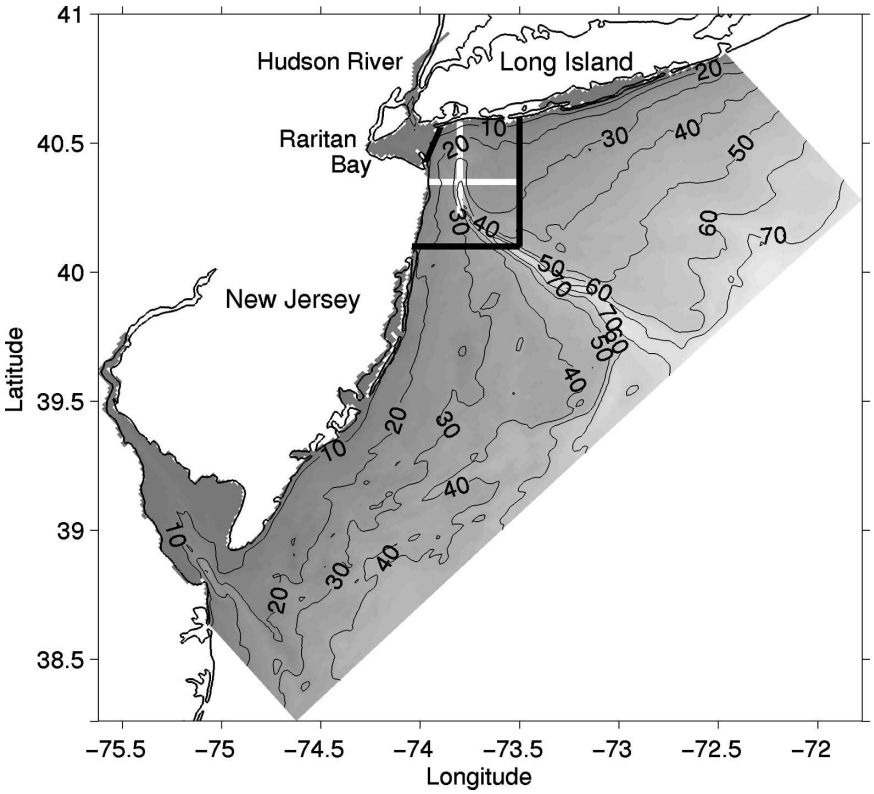

FIG. 2. Model domain and bottom topography (m). Depth is contoured every 10 m. Black solid lines are the locations of freshwater flux calculation in sections 3c and 4d. White solid lines (along 73.80°E and 40.35°N) are the locations of the vertical cross sections in section 3c and those of the momentum balance calculation in section 4c.

2005a; Wilkin and Lanerolle 2005; Wilkin 2006). Details of the ROMS computational algorithms are summarized by Shchepetkin and McWilliams (2005) and Warner et al. (2005b). Vertical turbulence closure is the level-2.5 scheme of Mellor and Yamada (1982).

The model domain is rectangular with a coastal wall on the northwestern side and three open boundaries (Fig. 2). The model horizontal resolution is approximately 1 km with 30 levels in the vertically stretched terrain-following ROMS *s* coordinate. The domain is limited to the continental shelf with a maximum depth of 80 m at the end of the Hudson Canyon. Most of the domain has depths shallower than 60 m. Open boundary conditions are simple Orlanski-type radiation augmented with tidal harmonic forcing (seven constituents) taken from a tidal simulation of the western Atlantic (Mukai et al. 2002). It was determined early in the study that without tidal mixing the flow that exits the estuary forms an unrealistically thin and fresh surface plume. Tidal forcing is retained in all simulations. A weak (less than 4 cm s^{-1}) southwestward mean flow occurs in this region (Beardsley et al. 1976; Beardsley and Boicourt 1981) but is not imposed here. Fong and Geyer (2002) show that this flow would augment dispersal of the plume toward the south in a manner similar to that of southward wind forcing. Our results will show that wind-driven currents are several times greater than this modest mean flow, so we avoid the complexity of imposing the effect (associated with the shelfwide pressure gradient) in the model open boundary conditions. During the spinup, air–sea heat and momentum fluxes are calculated by bulk formulas (Fairall et al. 1996, 2003) using the model sea surface temperature and sea level air temperature, pressure, and relative humidity from National Centers for Environmental Prediction (NCEP) reanalysis climatology and winds observed at Ambrose Light Tower (40.46°N, 73.83°W). The diurnal cycle of incoming shortwave radiation is specified analytically assuming no clouds.

b. Initializing a freshwater plume and inner-shelf stratification

To study the influence of wind on an established Hudson River plume, the model was spun up with a constant river discharge of 500 $m^3 s^{-1}$ and daily mean

winds for 1 January–27 April 2004. Initial temperature and salinity for the spinup were computed by a weighted least squares fit to historic January through March hydrographic profiles grouped according to water depth.

The anemometer at Ambrose Light Tower is at 21-m height, so the observed winds were scaled by a factor of 0.85 to get a 10-m wind for use over the shelf region of the domain. Smaller factors of 0.65 and 0.45 were used for the estuary (Raritan Bay and New York Bay) and Hudson River, respectively. These factors were estimated by comparing winds at Ambrose Light Tower with shipboard measurements during LaTTE 2004. The wind directions were kept as they were measured.

The model domain includes an idealized Hudson River estuary extending northward about 50 km from Raritan Bay. At the upper end of the modeled estuary, the imposed Hudson River volume flux (at zero salinity) enters a model cell, adding both volume and momentum. The momentum flux is distributed uniformly over the water column of 4-m depth, but in practice the added momentum is rapidly dissipated in the narrow model estuary. Hudson River temperature variability is specified from daily averaged river gauge measurements to the south of Hastings-on-Hudson [U.S. Geological Survey (USGS) stream gauge 01376304] during 2004.

During the model spinup an estuarine circulation develops in the estuary and river: low-salinity partially mixed water flows out at the surface and more saline shelf water intrudes into the estuary at depth. The plume behavior during spinup is consistent with the expectation of how a relatively low volume steady river flow advances into the coastal ocean; upon entering the open shelf the plume turns to the right and flows predominantly along the New Jersey coast. The horizontal pattern of plume dispersal is readily visualized in terms of the equivalent depth of freshwater δ_{fw}, defined as

$$\delta_{\mathrm{fw}} = \int_{-h}^{\eta} \frac{S_a - S(z)}{S_a}\, dz, \tag{1}$$

where S_a is an ambient or reference salinity (here S_a = 32.76) representative of the shelf water into which the plume flows, $S(z)$ is the salinity of the water column, η is sea level, and h is bottom depth. If the water column could locally be "unmixed" into two layers of salinity zero and S_a, the freshwater layer would be δ_{fw} thick. The distribution of equivalent freshwater depth at the conclusion of the spinup period is shown in Figs. 3a,c. Water discharged from the Hudson River is confined mostly near the New Jersey coast with relatively little freshwater along the coast of Long Island. The surface current is strongest along the boundary between inshore freshwater and offshore saline water (Fig. 3a), while offshore the surface velocity is weak. Approaching the end of the spinup, winds averaged about 2.2 m s^{-1} toward the west and caused some freshwater to accumulate in New York Bay and in the south of Raritan Bay (Fig. 3c). Winds dropped at the end of the spinup allowing this water to exit the estuary, and the freshwater transport from Raritan Bay to the New York Bight reached about 800 m^3 s^{-1} (i.e., exceeding the river flow of 500 m^3 s^{-1}). Therefore, the initial condition for the idealized forcing scenarios below is not an equilibrium response to steady forcing, but is simply a plausible initial condition during the low flow season after dispersal by realistically variable winds that have not dominated the plume dynamics.

3. Constant low discharge (500 m^3 s^{-1})

a. Unforced river plume (no wind)

For comparison with the forced scenarios, the evolution of the coastal circulation starting from the initial conditions described above is computed for continued river discharge of 500 m^3 s^{-1} but no wind forcing.

The freshwater previously accumulated in the estuary by the westward wind exits Raritan Bay and flows along the New Jersey coast (Fig. 3b). The southward current is stronger along the plume front than near the coast. The spatial pattern of surface currents is not appreciably different from the initial condition, but after 3 days the low-surface-salinity front has moved father southward along the New Jersey coast, and the area of the freshwater plume has expanded offshore. The freshwater volume decreases in the bay and increases along the New Jersey coast.

b. Response of plume to different wind directions

To examine the response of the Hudson River plume to different wind directions, moderate (5 m s^{-1}) winds are blown to each of the four compass points for 3 days starting from the same initial conditions. The wind speed is increased slowly from 0 to 5 m s^{-1} over 12 h to prevent inertial oscillation generation by an abrupt change of wind. Surface salinity, surface currents, and freshwater volume are compared in Fig. 4.

When northward wind blows, flow is toward the east at the mouth of Raritan Bay (Figs. 4a,e). Within 3 days the surface current takes freshwater from the bay and develops a broad low-salinity patch offshore from Long Island. Because the water leaving the bay mixes with ambient saline water during eastward advection its surface salinity increases, but this is the wind scenario that

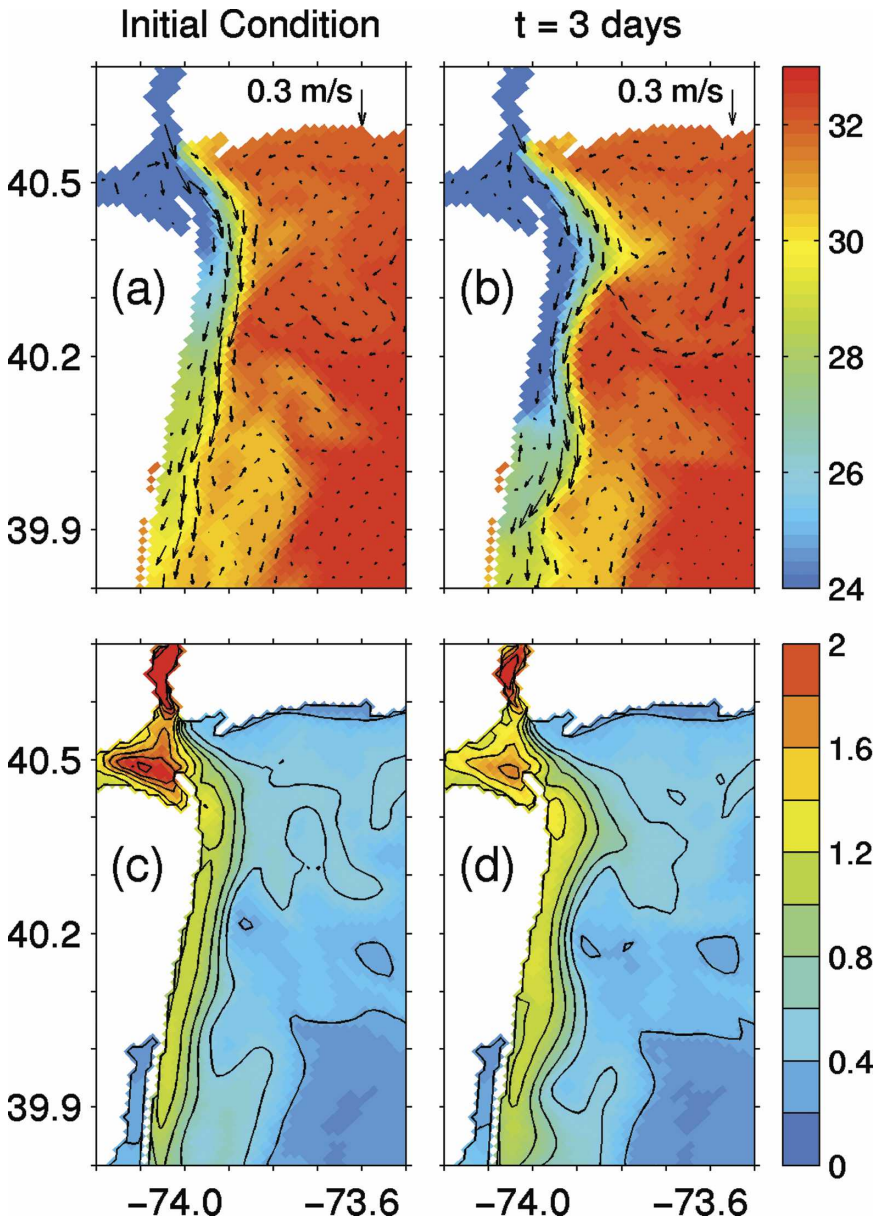

FIG. 3. (a), (c) Initial condition at $t = 0$; (b), (d) the unforced Hudson River plume at $t = 3$ days. The river discharge is steady and low at 500 $m^3 s^{-1}$. (top) Surface salinity and current vectors at 1-m depth, and (bottom) equivalent depth of freshwater δ_{fw} [m; contour interval (CI) is 0.2 m].

produces the freshest water along Long Island. Low-salinity water previously aligned along the New Jersey coast in the initial conditions (Fig. 3c) is moved offshore by Ekman transport to form a broad north–south freshwater band, consistent with the findings of Fong and Geyer (2002). To compensate for this eastward advection, subsurface saline water upwells along the New Jersey coast and flows northward.

Southward wind (Figs. 4b,f) drives surface Ekman flow toward the New Jersey coast, causing the coastal freshwater band to become more narrow and its thickness to increase. The southward coastal jet along the New Jersey coast is stronger in this case than for any other wind conditions and transports the most freshwater to the south. Southward wind generates westward flow along the Long Island coast and southwestward surface flow offshore, leading to the highest salinities in the north of any wind scenario.

Eastward wind is effective at pushing surface water out of Raritan Bay, and less freshwater remains in the

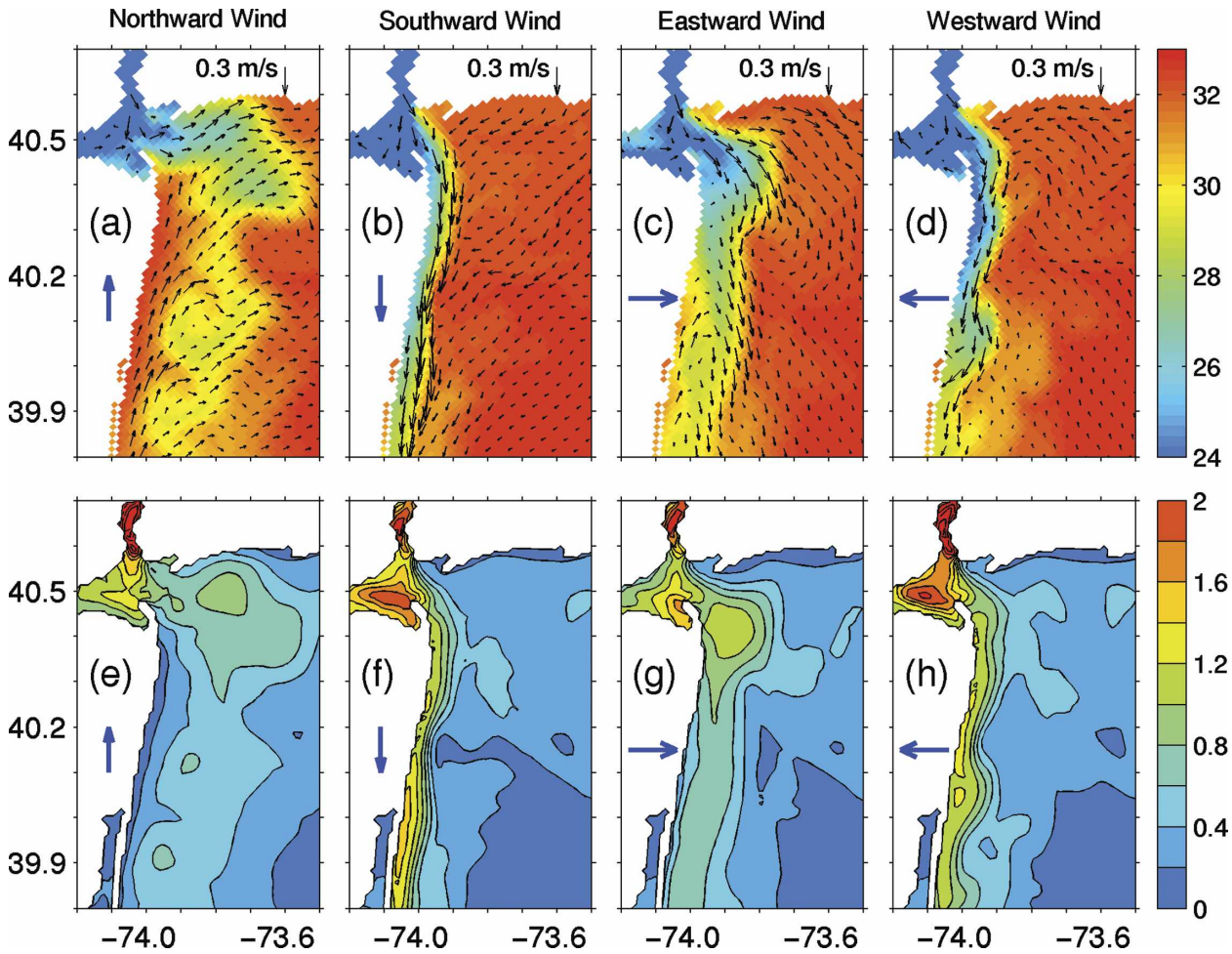

FIG. 4. Response of the Hudson River plume to different wind directions. (top) Surface salinity and current vectors at 1-m depth, and (bottom) equivalent depth of freshwater δ_{fw} (m) after 3 days of wind forcing (t = 3 days). The CI for δ_{fw} is 0.2 m. Winds of 5 m s^{-1} blow (a), (e) northward, (b), (f) southward, (c), (g) eastward, and (d), (h) westward. Blue arrow over the land indicates wind direction. The corresponding results with no wind forcing are shown in Figs. 3b,d.

bay than for other wind conditions (Figs. 4c,g). Upon leaving the bay the flow travels east and then south, forming a broad southward surface flow. The inshore surface currents are weak and the offshore southward surface flow is spread over a broad cross-shelf region separated from the New Jersey coast. This offshore southward surface current removes some freshwater to the south, but a substantial portion accumulates near the head of the Hudson shelf valley. Though the surface current does not recirculate, δ_{fw} shows a closed contour similar to the bulge pattern common for unforced surface-advected plumes, indicating that under these wind conditions the freshwater discharge is not dispersed far from the mouth of Raritan Bay. A strong eastward surface current develops along the Long Island coast, but it is not fed by low-salinity water leaving the estuary. There is a weak northward current along the New Jersey coast associated with a reversed geopotential gradient resulting from the initial low-salinity plume being displaced offshore.

Westward wind accumulates freshwater in Raritan Bay as is expected from studies showing the importance of wind that is parallel to the estuarine axis (Sanders and Garvine 2001; Janzen and Wong 2002). Enough freshwater exits the bay to sustain the coastal current along the New Jersey coast and the surface salinity and velocity there are similar to the unforced plume case. The surface current along the surface salinity front is weak relative to the southward and eastward wind conditions, while close to shore the southward currents are somewhat stronger. Surface current along the Long Island coast is weakly westward.

Associated with the wind-driven changes in the horizontal dispersal of the plume are changes in the vertical

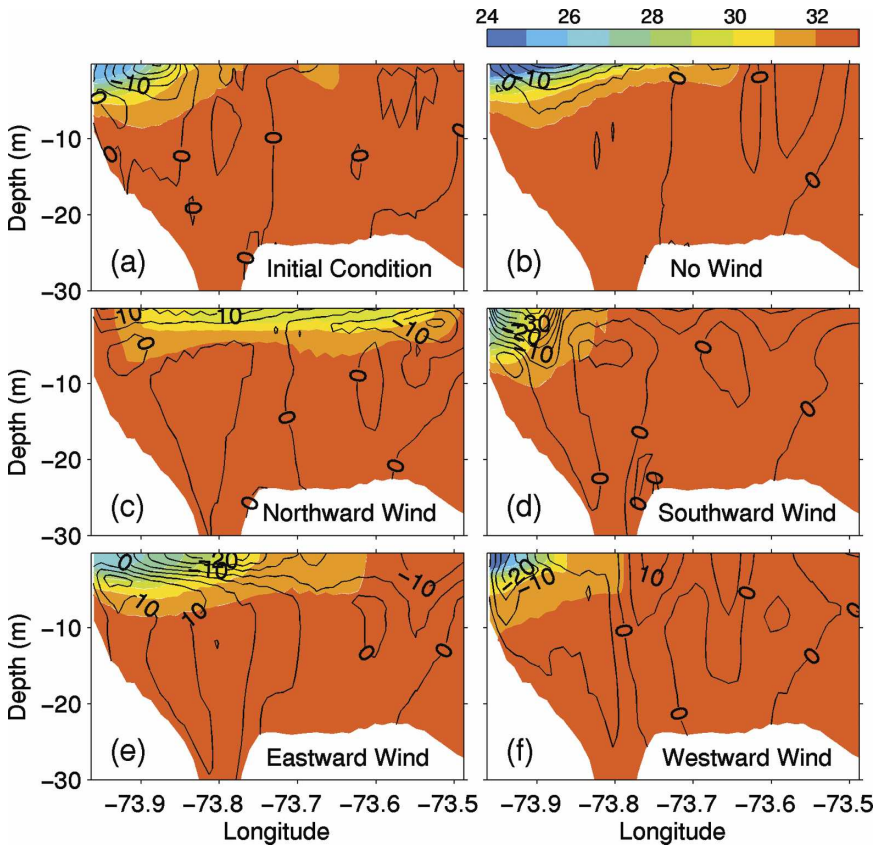

FIG. 5. For low-discharge scenarios, the salinity (color) and northward component of the current (contours) across a section along 40.35°N. (a) Initial condition, (b) the unforced plume at day 3, and after 3 days of 5 m s^{-1} wind forcing toward the (c) north, (d) south, (e) east, and (f) west. Currents: cm s^{-1}; CI: 5 cm s^{-1}.

distribution of salinity and velocity across the New Jersey coast. Figure 5 compares salinity and northward velocity sections for the different wind scenarios along 40.35°N from the New Jersey coast (73.98°W) to 40 km offshore (73.5°W). The cross-shore section is about 12 km south of Raritan Bay mouth.

In the initial conditions the coastal plume is 17 km wide and 8 m thick (Fig. 5a). Here plume water is defined as any water with salinity less than 32. The lowest salinity of the initial plume is 24.8. Without wind forcing for 3 days, the plume expands to the east as it relaxes from the influence of prior wind forcing and is fed with new freshwater from Raritan Bay. The unforced plume becomes 28 km wide, with the offshore part of the plume being only 3 m thick. The lowest salinity of the unforced plume is 17.6 because the new water joins the plume without being mixed downward by surface winds.

After 3 days of northward upwelling-favorable wind, surface freshwater from the initial plume is spread offshore in an approximately 6-m-thick layer with surface salinity of 29.1 (Fig. 5c). After southward winds, fresher water is squeezed against the coast, the plume width decreases to 13 km, and its thickness increases to about 10 m. The strong southward coastal jet has a surface speed of about 40 cm s^{-1} along the salinity front.

When the eastward wind blows the coastal plume expands 30 km offshore, about as far as the unforced plume, but the halocline is deeper (9 m) because of vertical mixing. The center of the southward flow is about 12 km offshore while the core of freshwater is still attached to the coast. Surface flow is northward within 3 km of the coast, and for the subsurface flow (below 3 m) there is a northward current from the coast out to 22 km offshore. For this eastward wind scenario the subsurface northward current is actually stronger than that in the case of the directly northward wind. During winter unstratified conditions, eastward winds have been found to drive flow up the Hudson shelf valley at depth to feed offshore surface transport (Harris et al. 2003). The southward flow that is displaced offshore (Fig. 4c) is likely to entrain northward flow

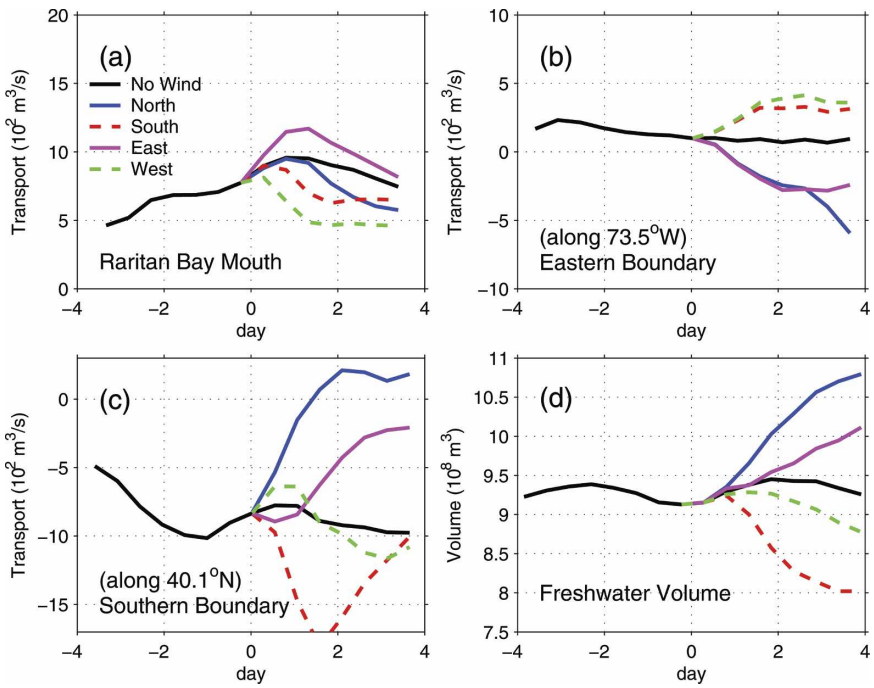

FIG. 6. Low river discharge scenario freshwater transport into the New York Bight apex through (a) Raritan Bay mouth, (b) eastern boundary (along 73.5°W), (c) southern boundary (along 40.1°N), and (d) integrated freshwater volume within the domain. Positive (negative) transport implies freshwater volume transport into (out of) the domain.

from near the coast that is driven by the geopotential gradient in the halocline depth.

Westward wind pushes the plume to the New Jersey coast and it becomes about 15 km wide and 10 m thick. The core salinity is 23.3, which is the second freshest water next to the unforced plume. Southward velocity is strongest near the coast at 20 cm s^{-1} and has a subsurface intensification from 3 to 7 m.

c. *Freshwater budget in the New York Bight apex during steady low river discharge*

To quantify and more directly compare the effect of wind scenarios on freshwater dispersal and storage in the apex of the New York Bight, freshwater transports are estimated through the mouth of Raritan Bay, an eastern section (along 73.5°W), and a southern section (along 40.1°N), which encompass a closed volume. Freshwater volume transport V_{fw} is estimated by

$$V_{\mathrm{fw}} = \int \int_{-h}^{\eta} \frac{S_a - S}{S_a} u \, dz \, dx, \qquad (2)$$

where u is horizontal velocity normal to the section and the integral with respect to x is the horizontal distance across the section. We use for S_a the maximum value of modeled salinity in the region that ensures δ_{fw} is always positive and V_{fw} is positive in the direction of flow. If bottom salinities were significantly diluted in parts of the New York Bight then these values could be misestimated, but in our simulations this is not the case and our results in terms of equivalent freshwater depth and transport are robust. Time series of the section transports and integrated freshwater in the enclosed volume are plotted in Fig. 6.

Eastward wind increases freshwater export through the mouth of Raritan Bay, and westward wind decreases it, relative to the no-wind condition (Fig. 6a). Westward and southward winds have positive freshwater flux (inflow) through the eastern boundary (Fig. 6b), indicating that westward currents there bring in water of, on average, a lower salinity than that of S_a. Conversely, when currents turn eastward during eastward and northward winds the freshwater transport is to the east. Southward wind most effectively removes freshwater to the south through the southern boundary, while northward and eastward winds rapidly reduce the southward freshwater transport (Fig. 6c). Time series of freshwater volume in the New York Bight apex diverge under different wind scenarios (Fig. 6d). The net effect of the transports through the boundary sections is that northward wind increases the freshwater volume by spreading freshwater offshore of Long Island; eastward

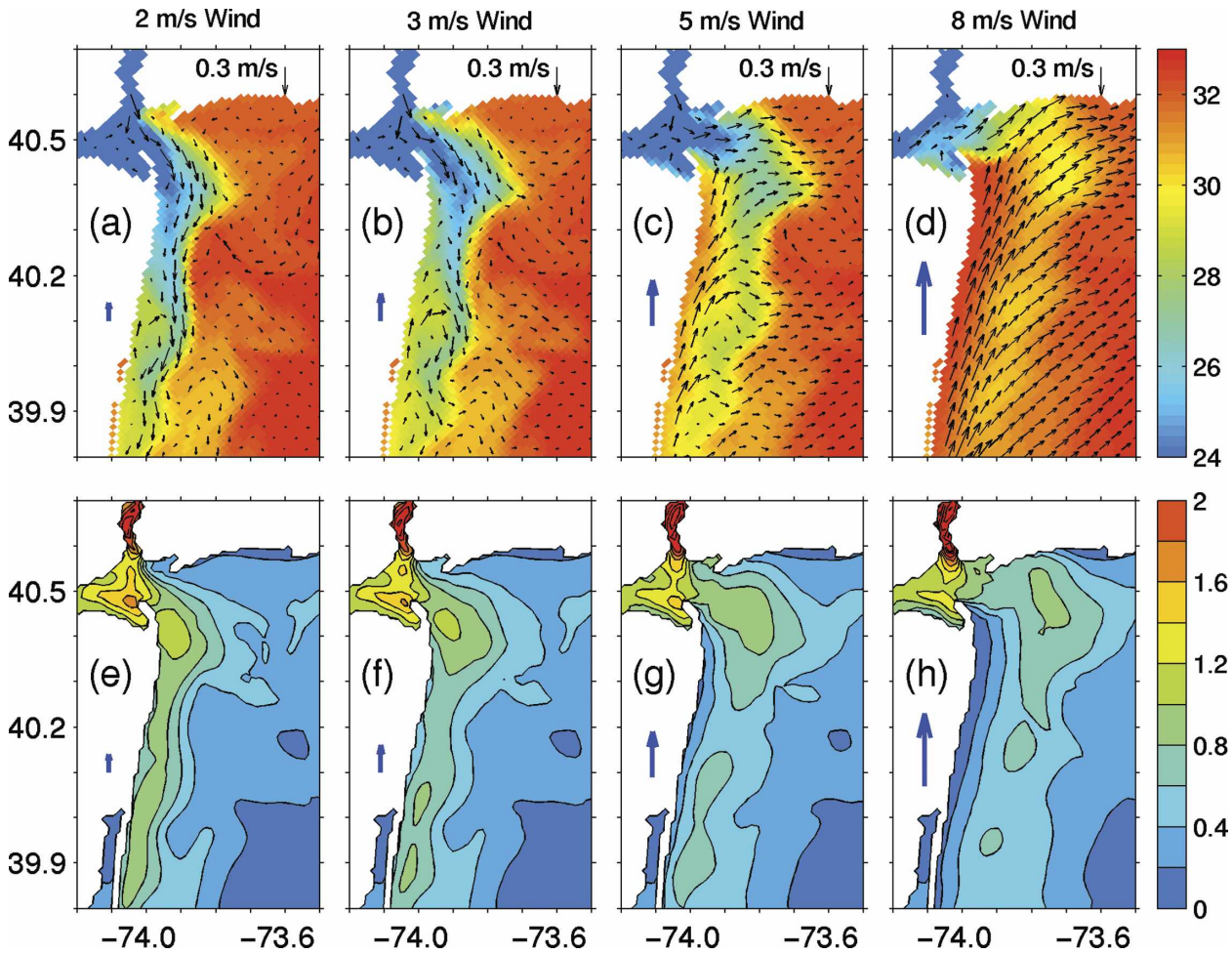

FIG. 7. The Hudson River plume after 2 days of northward wind forcing of speed of (a), (e) 2, (b), (f) 3, (c), (g) 5, and (d), (h) 8 m s^{-1}. (top) Surface salinity and current vectors at 1-m depth, and (bottom) equivalent depth of freshwater (m; CI is 0.2 m). Blue arrow over the land indicates wind speed and direction.

wind increases it by accumulating freshwater in a freshwater bulge at the south of Raritan Bay mouth; westward wind decreases it by accumulating freshwater within Raritan Bay and having less freshwater exit the estuary; and southward wind rapidly decreases it by draining freshwater along the New Jersey coast.

d. Response of plume to different wind stress

Northward wind [the upwelling-favorable case considered by Fong and Geyer (2002)] has the greatest impact on the southward transport of the coastal current and the storage of freshwater in the New York Bight apex. To examine how this response differs with wind magnitude, northward wind is blown with speeds of 2, 3, 5, and 8 m s^{-1} for 2 days (Fig. 7). These wind speeds correspond to stresses of 0.006, 0.013, 0.035, and 0.090 Pa, respectively. River discharge is kept at 500 m^3 s^{-1}. The wind blows northward in these simulations.

As a weak northward wind of 2 m s^{-1} blows for 2 days, freshwater leaves Raritan Bay and flows along the New Jersey coast, but is spread farther offshore than in the initial condition. The surface offshore velocity is weak. When the wind is increased to 3 m s^{-1} the plume lies farther eastward and the main freshwater stream becomes detached from the New Jersey coast. Salinity along the New Jersey coast is greater because salty water upwells to replace the surface freshwater displaced offshore. South of Long Island surface water starts to move eastward. At 5 m s^{-1} (less than 10 kt) surface water is pushed eastward out of Raritan Bay and flows parallel to the coast of Long Island. The plume that previously lay along the New Jersey coast is clearly detached and forms a north–south band of low-salinity water offshore. The surface current over the previous plume is eastward consistent with Ekman dynamics (2 days is 2.6 inertial periods since the onset of the wind).

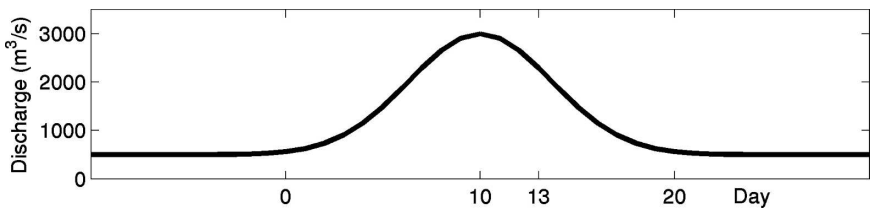

FIG. 8. River flow rate during the idealized high-discharge event. Background discharge is 500 $m^3 s^{-1}$ and the maximum is 3000 $m^3 s^{-1}$.

Saline water is being upwelled all along the New Jersey coast and transported northward in a coastal jet. When the wind is a stiff 8 m s^{-1} freshwater is driven out of Raritan Bay and along the Long Island coast. As the estuary discharge flows to the east vigorous vertical mixing increases the surface salinity, though the pattern of equivalent freshwater depth indicates that the net horizontal dispersal is not appreciably different from the 5 m s^{-1} case. The low surface salinity of the original plume is all but obliterated. Strong northward flow develops in a band confined within 15 km of the New Jersey coast.

4. High-discharge event (maximum 3000 $m^3 s^{-1}$)

The Hudson River has high-discharge events during the spring snowmelt (the freshet) and storms with heavy precipitation (Fig. 1). Events last about 20 days and the maximum discharge can exceed 3000 $m^3 s^{-1}$. To simulate an idealized high-discharge event comparable to the strong spring freshet during LaTTE 2005, a Gaussian shape for the river discharge time series is assumed starting from 500 $m^3 s^{-1}$, increasing to 3000 $m^3 s^{-1}$ over 10 days, and then decreasing back to 500 $m^3 s^{-1}$ during the next 10 days (Fig. 8). Simulations of the plume during the high-discharge event without wind forcing are presented first (section 4a) for comparisons with simulations where the wind is directed toward each of the four compass points (section 4b).

a. Unforced high-discharge event (no wind forcing)

The longitudinal distance that salt intrudes into the Hudson River estuary varies significantly with river discharge (Warner et al. 2005a). For the first 6 days of the high river discharge event the upper 3 m of the water column flows southward and is fed by both the river discharge and weak upstream transport of salty water. This estuarine circulation reaches to within 5 km of the modeled river source. When river discharge is near its maximum of 3000 $m^3 s^{-1}$ from days 7 to 12, the upper layer of low-salinity water deepens and the salt intrusion retreats southward some 15–20 km to lie near 40.7°N. The salt intrusion advances north of 40.8°N when the discharge returns to 500 $m^3 s^{-1}$. These features of estuarine variability are consistent with observations and a much higher resolution model of the Hudson estuary (Warner et al. 2005a).

As river discharge increases without wind forcing, freshwater initially accumulates within Raritan Bay then begins to extend eastward. By the time the discharge reaches its maximum of 3000 $m^3 s^{-1}$ (10 days later) (Figs. 9a,e), a low-salinity bulge (somewhat elongated north–south) has formed outside the mouth of Raritan Bay. A weak northward current develops at the western inshore side of the bulge along the northern New Jersey coast. The freshwater jet leaving Raritan Bay feeds the eastern edge of the bulge.

The lower Hudson River, New York Bay, and Raritan Bay accumulate freshwater within their basins, so there are time lags in freshwater volume transport at the land end of the freshwater source in comparison with the mouth of Raritan Bay. At day 10, when the river discharge is 3000 $m^3 s^{-1}$ at the model's nominal Hudson River source 50 km upstream from Raritan Bay, freshwater transport through Raritan Bay mouth is about 1900 $m^3 s^{-1}$. Though river discharge decreases from day 10 onward, the surface water in Raritan Bay continues to freshen until day 17.

As predicted by Fong and Geyer (2002), at high-discharge rates the coastal current cannot match the river flow and the freshwater bulge southeast of the mouth of Raritan Bay accumulates freshwater within an anticyclonic recirculation. The surface velocity is strongest on the offshore side of the bulge where the newly discharged water joins the recirculation. Not until day 16 does the bulge appear to rupture and allow freshwater to drain to the south along the New Jersey coast (Figs. 9c,d,g,h).

b. Response of the high-discharge plume to different wind directions

Following an approach similar to that in section 3b, the effect on the plume of different wind directions is considered next. The wind forcing commences on day

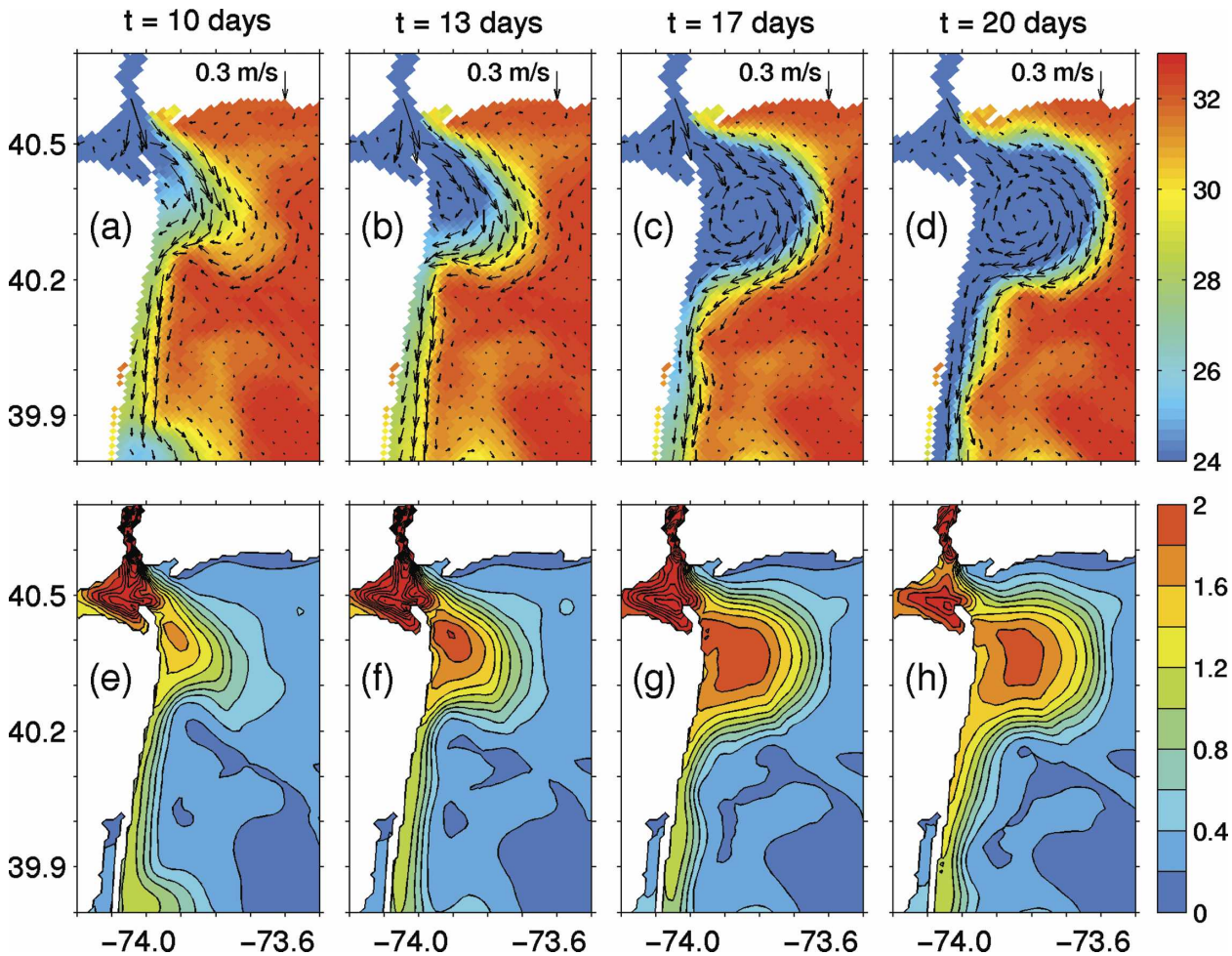

FIG. 9. Freshwater bulge formation and rupture to the south during the unforced high river discharge event. (top) Surface salinity and current vectors at 1-m depth, and (bottom) equivalent freshwater depth (m; CI is 0.2 m).

10 when the river discharge is at its maximum, and is then held steady at 5 m s^{-1} in all experiments. This choice of wind speed was made in light of the results of section 3d showing that 5 m s^{-1} forcing significantly affects the buoyancy-driven plume dynamics without overwhelming them. The speed is typical of wind variability in the region.

As compared with the unforced plume at day 13 (Figs. 9b,f), northward wind moves the accumulated freshwater (the previous plume) in the bulge toward the northeast and drives a new plume from Raritan Bay parallel to the Long Island coast (Figs. 10a,e), but the flow is not as close to Long Island as in the low-discharge scenario (Fig. 4a). The eastward surface current is fastest over the northern part of the plume and the recirculation on the southern part of the freshwater patch is weak. Saline water upwells along the New Jersey coast in a band about 8 km wide and flows northward. The vestiges of the previous coastal plume are seen in the band of low-surface salinity offshore.

Of all wind directions, the southward wind case has the greatest similarity to the corresponding low-discharge scenario (Figs. 4b,f). Southward wind pushes the constriction in flow at the southwest corner of the unforced bulge down the coast to near 40.2°N (30 km south of the mouth of Raritan Bay), and to the south of this there is a strong coastal jet along the New Jersey coast. The coastal jet drains freshwater from the bulge, drawing the maximum in the equivalent freshwater depth to the coast and eliminating the region of northward flow that previously closed the recirculation. The reservoir of freshwater stored in the New York Bight apex is smallest for this wind condition.

Eastward wind is again more effective at pushing freshwater out of Raritan Bay than any other wind con-

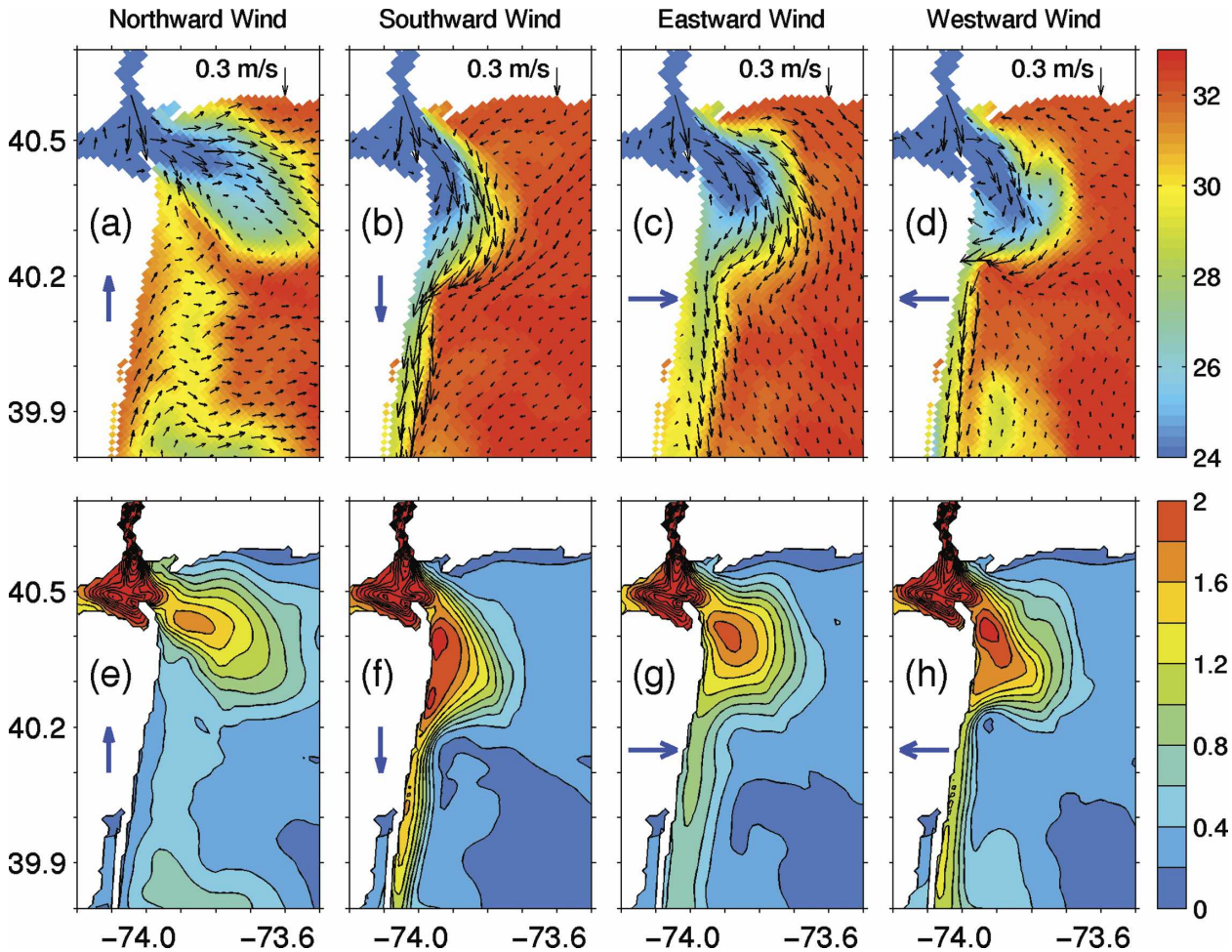

FIG. 10. Response of the Hudson River plume to wind direction during a high river discharge event. (top) Surface salinity and current vectors at 1-m depth, and (bottom) equivalent depth of freshwater δ_{fw} (m) 3 days after wind commences. The CI for δ_{fw} is 0.2 m. Winds of 5 m s^{-1} blow (a), (e) northward, (b), (f) southward, (c), (g) eastward, and (d), (h) westward. Blue arrow over the land indicates wind direction.

dition. While eastward winds blow, surface freshwater exits Raritan Bay and flows to the southeast to feed the preexisting bulge. The broad surface currents turn clockwise to join a southward alongshore current at 40.2°N (Figs. 10c,g). The northward recirculation at the coast is weak, but still present. The increased flow in the coastal jet south of 40.2°N is sufficient to prevail over the weak northward flow that arose along the south Jersey coast in the low-discharge eastward wind scenario.

Westward wind accumulates more freshwater and produces lower surface salinity in Raritan Bay than the other wind conditions (Figs. 10d,h). The freshwater bulge becomes elongated and distorted and is seemingly bisected by the southward current that is fed by the estuary discharge. A further distinctive feature of the surface velocity is that the eastern part of the freshwater bulge has very weak or no surface current, suggesting that Ekman currents virtually cancel out the density-driven circulation around the bulge. A strong westward current develops at the south of the bulge (40.25°N) that pushes the freshwater against the coast (Fig. 10h) before bifurcating into the southward coastal jet and northward recirculation.

c. *Momentum balance in the plume*

To examine the vertical structure of the plume and identify the terms in the cross-shore momentum balance that are pertinent to the plume behavior, vertical sections through the major body of freshwater (along either 40.35°N or 73.80°W) are analyzed. Each section is from the coast to 40 km offshore, and 30 m deep. The vertical structure along 40.10°N will also be described,

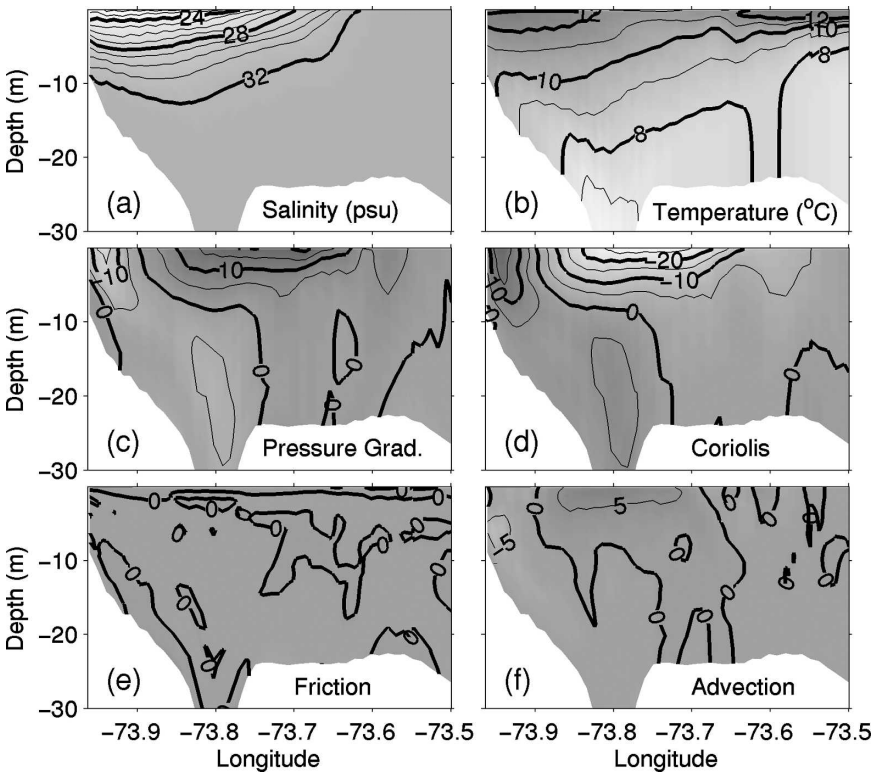

FIG. 11. Unforced plume, high-discharge event, vertical structure along 40.35°N from the New Jersey coast to 40 km offshore at day 13: (a) salinity and (b) temperature, and terms in the cross-shore (east–west) momentum balance: (c) pressure gradient, (d) Coriolis (fv), (e) friction, and (f) advection. CIs are salinity: 1, temperature: 1°C, and momentum: 5×10^{-6} m s^{-2}.

but the related figures are not shown. ROMS computes terms in the momentum equations on every time step and averages these over a chosen time interval to enable exact momentum diagnostics. The results shown in Figs. 11–15 are averages over an M_2 tidal period (12.4 h). The sign convention for all terms is that they are on the right-hand side of the momentum equation.

In the unforced plume experiment the anticyclonic bulge that recirculates low-salinity water in the apex of New York Bight is about 12 m deep and 31 km wide along 40.35°N at day 13 (i.e., 3 days after the river flow peaks) (Fig. 11). Surface salinity is about 22 and temperature is 12°C near the coast. A shallow warm layer over a strong vertical temperature gradient develops 32–40 km offshore because there is no wind stress to vertically mix the water column. The Coriolis parameter f is close to 10^{-4} s^{-1} at this latitude, so the 5×10^{-6} m s^{-2} contour intervals in the Coriolis term (fv) (Fig. 11d) correspond to 5 cm s^{-1} of northward velocity. The northward countercurrent ($v > 0$) is confined within 6 km of the coast, while elsewhere the surface current is southward. The force balance is predominantly geostrophic between the Coriolis term and the pressure gradient established by the low-density, low-salinity water. Nonlinear momentum advection (Fig. 11f) contributes where the current is strongest on the eastern side of the bulge. There the Rossby number (Ro; ratio of the advection to the Coriolis terms) is about 0.3, indicating a significant cyclostrophic balance.

South of the freshwater bulge at 40.10°N in Fig. 9b where the southward low-salinity coastal current is about 10 m deep and 12 km wide (results not shown), the surface salinity of the plume is 27 near the coast and increases steadily offshore. The center of the coastal jet is faster than 40 cm s^{-1} at the surface, but the balance is again geostrophic with a small contribution from the advection term (Ro = 0.1) because there is little curvature in the flow.

A section along 73.80°W (Fig. 12) shows the freshwater that moves toward Long Island in a layer about 12 m deep during northward wind, and its northern edge just touches the Long Island coast. The cross-shore (north–south) momentum balance is again predominantly geostrophic, but with the added influence of the northward wind stress appearing in the friction term distributed over a shallow surface fric-

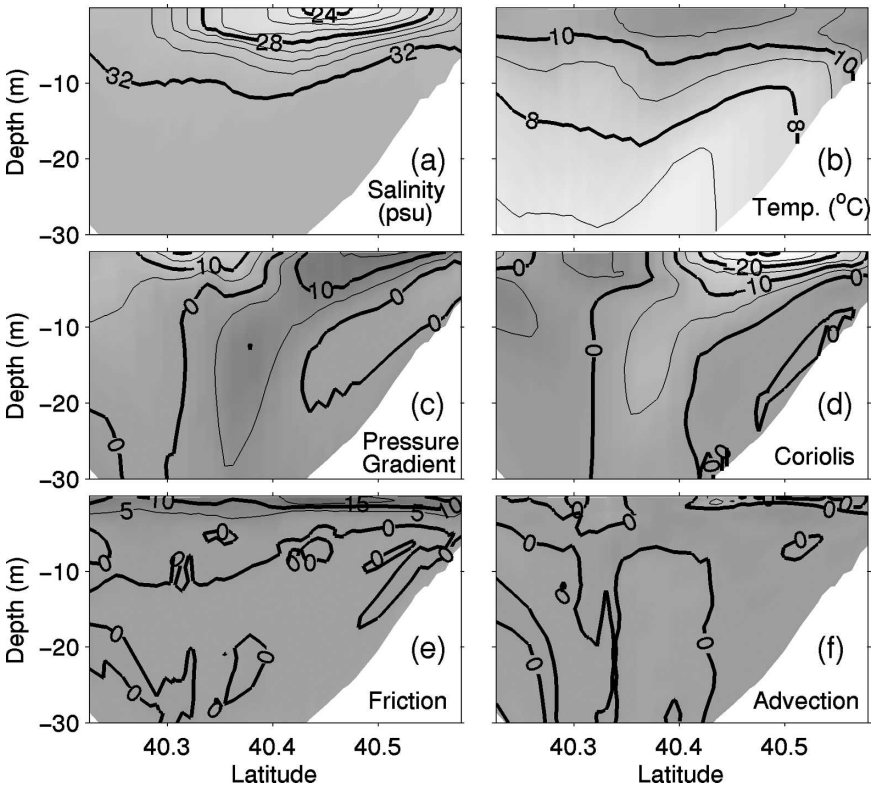

FIG. 12. Northward wind (5 m s^{-1}), high-discharge event, vertical structure along 73.80°W from 40 km offshore to the Long Island coast 3 days after the onset of winds: (a) salinity and (b) temperature, and terms in the cross-shore (north–south) momentum balance: (c) pressure gradient, (d) Coriolis ($-fu$), (e) friction, and (f) advection. CIs are as in Fig. 11.

tional boundary layer. Despite the wind speed being constant, Fig. 12e shows that the downward transfer of the momentum input (wind stress) varies spatially. The downward penetration of wind stress depends on vertical stratification of the water column. The thin surface layer close to Long Island where the Coriolis term is less than -25×10^{-6} m s^{-2} (or the eastward velocity is greater than 25 cm s^{-1}) indicates that the Ekman currents add some 15 cm s^{-1} eastward to the surface velocity. Presumably, this strong vertical shear in the velocity could aid the dilution of the freshwater anomaly by shear dispersion and vertical mixing. South of 40.41°N the Ekman currents are opposed by westward geostrophic velocity resulting in a weak surface flow.

Southward wind squeezes the freshwater bulge against the New Jersey coast and the low-salinity region becomes about 12 m deep and 23 km wide at the 40.35°N section (Fig. 13). Surface salinity is 24 and temperature is 12°C at the coast. Offshore the wind mixed layer is about 7 m deep. The southward current is strongest along the plume front (surface speed greater than 30 cm s^{-1} at 73.8°W) and is in geostrophic balance (Figs. 13c,d). Momentum advection is significant only in the core of the southward jet, but plays a modest role in the net force balance (Ro = 0.15). Winds are alongshore, so friction does not contribute to the cross-shore momentum balance here, but the effects of westward Ekman transport can be seen in the downwelling of temperature immediately adjacent to the New Jersey coast. At 40.10°N, south of the bulge in Fig. 10b, the coastal plume is tightly attached to the New Jersey coast and is about 7 km wide and 13 m deep, with a surface salinity of 28 and a temperature of 11°C near the coast (not shown). The coastal jet exceeds 60 cm s^{-1} at the center but remains predominantly geostrophic (Ro = 0.06).

Eastward wind produces a freshwater bulge of a similar depth (12 m) to the southward wind case, but a greater width (34 km) (Fig. 14), consistent with the observation in section 4b that the reservoir of freshwater stored in the New York Bight apex is smallest for southward wind. Winds vertically mix the upper water column (to about 7-m depth) so that, as in the southward wind case, surface waters are saltier and cooler than for the unforced plume. Where the buoyancy

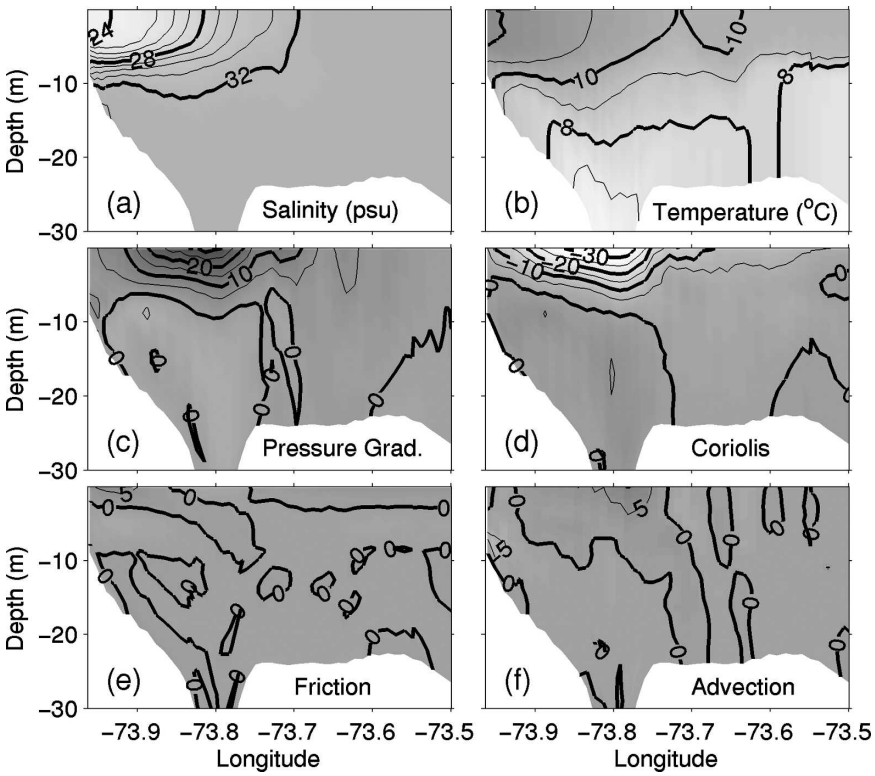

FIG. 13. Southward wind (5 m s^{-1}), high-discharge event, vertical structure along 40.35°N from the New Jersey coast to 40 km offshore 3 days after the onset of winds: (a) salinity and (b) temperature, and terms in the cross-shore (east–west) momentum balance: (c) pressure gradient, (d) Coriolis, (e) friction, and (f) advection. CIs are as in Fig. 11.

anomaly and contours of the equivalent freshwater depth take a maximum in the bulge (Fig. 10g) corresponds to the change in sign of the pressure force in the cross section (Fig. 14c). Geostrophic velocity is therefore northward from the coast to 9 km offshore, and southward farther east. Where southward Ekman velocity augments southward geostrophic velocity on the eastern side of the bulge there are strong southward surface currents. The subsurface maximum of northward current near the coast (4–7-m depth) results from superposition of strong northward geostrophic velocity (25 cm s^{-1}) and opposing southward Ekman velocity (15 cm s^{-1}) from the surface to 4-m depth. With some similarities to the unforced case, there is a moderately strong subsurface geostrophic northward flow up the axis of the Hudson shelf valley below 8-m depth beneath the center of the bulge. As noted earlier, circulation in this direction during eastward winds occurs in wintertime observations of currents in the axis of the shelf valley (Harris et al. 2003).

Under the influence of westward winds the freshwater bulge at 40.35°N is of comparable depth (11 m) and width (28 km) to that of the other wind-forced cases (Fig. 15). The Ekman velocity that would balance the negative friction term from westward wind stress (Fig. 15e) is now northward in opposition to the southward buoyancy-driven flow from the high river discharge. However, it is not sufficient to overcome the pressure gradient, so the flow is weakly southward near the surface but much stronger at depth away from influence of the winds. The subsurface maximum (5-m depth) in southward velocity is very strong (greater than 25 cm s^{-1}), being aided by significant curvature in the flow at 73.85°W (Fig. 10d) that produces a moderate contribution from the advection term (Ro = 0.25). This is interesting in the respect that it highlights that the surface-only observations of current, such as from a Coastal Ocean Dynamics Application Radar (CODAR) system, might indicate little transport in the bulge when in fact there is substantial southward transport of low-salinity water masked by Ekman dynamics.

On the west side of the surface salinity minimum the pressure force is reversed and Ekman transport augments northward geostrophic velocity from the coast to 4 km offshore to form a recirculating flow on the inshore side of the bulge.

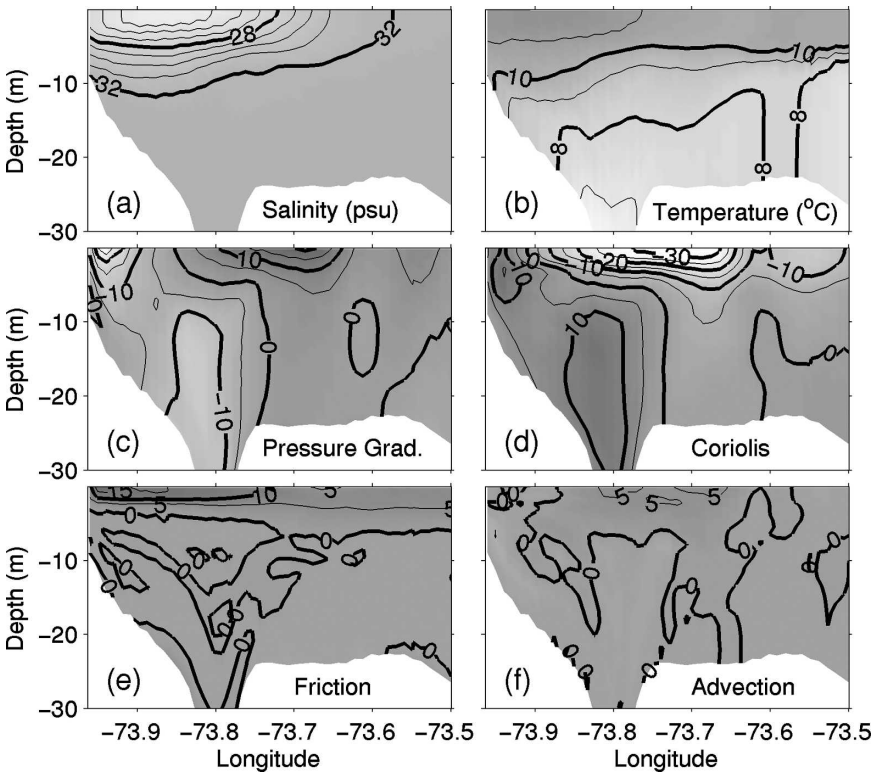

FIG. 14. As in Fig. 13, but for an eastward wind.

d. Freshwater budget in the New York Bight apex during a high-discharge event

Following the approach used in section 3c, the effect of wind on the dispersal of a high river discharge event is examined by considering freshwater transport through sections that enclose the apex of the New York Bight. At day 10 of the high-discharge event, when the river inflow is at a maximum, freshwater input into the New York Bight through the mouth of Raritan Bay is about 1800 $m^3\ s^{-1}$ and across the eastern boundary of the region (73.5°W) about 100 $m^3\ s^{-1}$. At this time freshwater is leaving the region of interest to the south along the coast at 800 $m^3\ s^{-1}$. This imbalance of transports at day 10 means the freshwater volume within the New York Bight apex is growing at approximately 1100 $m^3\ s^{-1}$. In the unforced scenario this convergence of transport causes the freshwater bulge to grow, even as the river discharge declines. In the forced scenarios the onset of winds occurs at day 10, causing the time series of freshwater storage and dispersal to evolve differently from the unforced case.

When eastward winds blow, freshwater is flushed into the New York Bight from Raritan Bay more rapidly than in the no-wind case during days 10–16 (Fig. 16a). Westward winds obstruct freshwater from leaving the bay, whereas northward and southward winds allow about the same amount of freshwater to exit the bay as in the no-wind condition.

For northward winds, freshwater entering the New York Bight spreads out to the east and export through the eastern boundary steadily increases (Fig. 16b). Meanwhile, the coastal current transport across the southern boundary quickly falls to zero (Fig. 16c) so that the increase in integrated freshwater volume within the region is arrested at day 15 and the bulge begins to drain. Southward wind quickly increases the southward freshwater flow to 2000 $m^3\ s^{-1}$ within 3 days of wind forcing without significantly impacting the other boundaries. Consequently, the bulge immediately decreases in volume. As noted previously, southward wind is the most efficient at removing the discharged river waters from the apex of the bight.

Westward winds somewhat strengthen the transport of freshwater out through the southern boundary (relative to the no-wind case) but compensate with a comparable modest increase in inflow from the east. Nevertheless, the rate of increase of freshwater storage initially declines, not only because previously discharged river water is being dispersed, but also because the inflow from Raritan Bay was interrupted. This hiatus can-

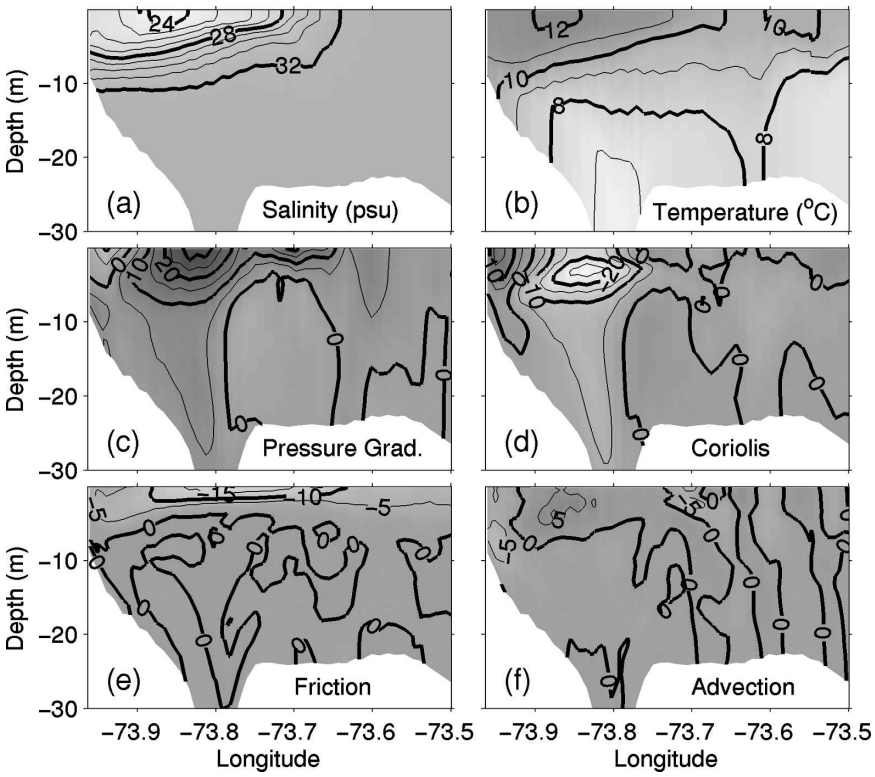

FIG. 15. As in Fig. 13, but for a westward wind.

not be sustained, and by day 18 the integrated freshwater volume within the region decreases and is overtaken by the unforced case. Eastward winds grow the largest freshwater bulge in this high-discharge scenario and freshwater volume in the New York Bight apex continuously increases (Fig. 16d).

5. Summary

This study investigates the influence of winds on the dispersal of the Hudson River plume for two river discharge scenarios that characterize typical flow conditions; namely, a steady low- and a high-discharge event resembling the spring freshet. Wind direction and strength affect freshwater transport through the estuary mouth and the subsequent path that the plume takes in the waters of New York Bight. The modeled plume was initialized by simulating coastal circulation using observed daily winds for the first quarter of 2004 and steady river discharge close to the annual mean (500 $m^3\ s^{-1}$). The initialization was intended merely as a plausible initial state from which the perturbation of a controlled set of wind forcing scenarios could begin.

In the first set of simulations, wind is directed toward the four compass points while the low river discharge is maintained. Northward wind causes the initial plume, which would otherwise have continued to flow along the New Jersey coast in the absence of wind, to drift to the east and spread out in a thin (6 m) low-salinity layer. Saline subsurface water upwells along the New Jersey coast and flows northward. A new plume of water discharged from Raritan Bay flows along the Long Island coast. Southward wind pushes the plume against the New Jersey coast and the plume thickens. A strengthened coastal jet drains freshwater to the south along the coast. Eastward wind enhances freshwater export from the estuary into the New York Bight and accumulates low-salinity water in an anticyclonic bulge in the apex of New York Bight. Surface currents flow southeastward over the northeastern part of the bulge, and then join a southward flow that is detached from the coast. Westward wind retards freshwater export through the estuary mouth and squeezes the plume toward the New Jersey coast, with the structure of the coastal current and freshwater transport along the coast being similar to the unforced plume.

A high river discharge event is simulated with flow that grows from a low background value (500 $m^3\ s^{-1}$) to a peak of 3000 $m^3\ s^{-1}$ over the course of 10 days, and

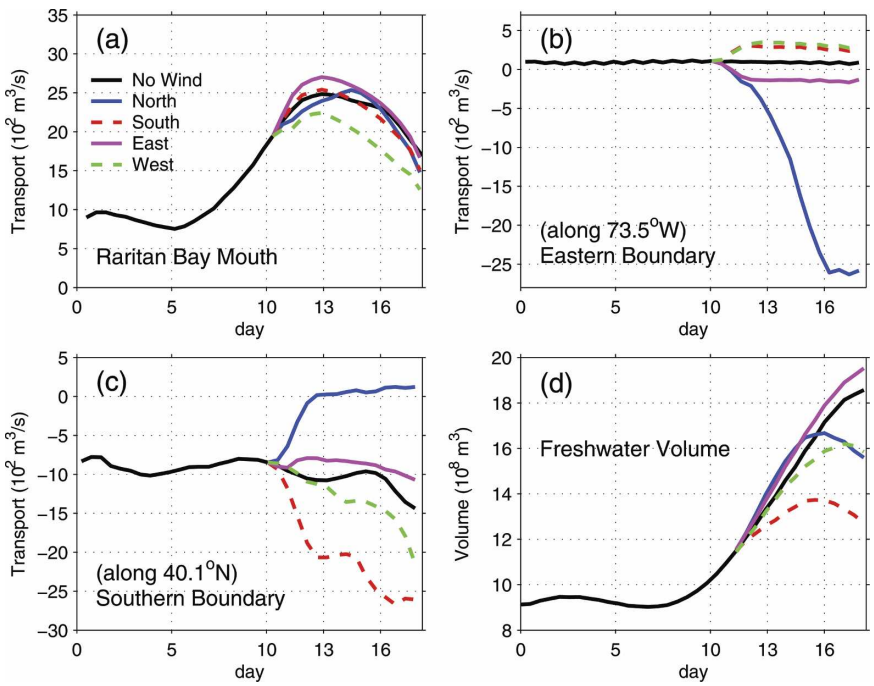

FIG. 16. High-discharge event freshwater transport into the New York Bight apex through (a) Raritan Bay mouth, (b) eastern boundary (along 73.5°W), (c) southern boundary (along 40.1°N), and (d) integrated freshwater volume within the region. Positive (negative) transport implies freshwater volume transport into (out of) the domain.

returns to low flow over the following 10 days. While the modeled freshet is growing no winds are imposed and a large freshwater bulge forms outside the mouth of Raritan Bay, both consistent with theories for the behavior of a surface-advected plume at high discharge (Yankovsky and Chapman 1997) and in good qualitative agreement with observations from the 2005 LaTTE program (Chant et al. 2006). If the high-discharge event concludes without wind forcing, freshwater export from Raritan Bay reaches a maximum of 2500 m^3 s^{-1} at day 13 and the freshwater bulge continues to grow and recirculate freshwater well beyond day 20.

Scenarios examining the effect of wind direction impose 5 m s^{-1} winds starting at day 10. Northward wind displaces the bulge eastward and redirects Raritan Bay outflow toward the Long Island coast. The combination of geostrophic and Ekman velocity on the north side of the displaced bulge efficiently sweeps freshwater eastward away from the apex of the New York Bight. Even more effective at draining the bulge is southward wind, which promptly shuts down the northward recirculation and accelerates the southward New Jersey coastal current.

Eastward wind moderately increases the initial export of freshwater from Raritan Bay but also increases the flux of freshwater away to the east. The overall effect is to accumulate slightly more freshwater in the bulge than in any other wind condition, including the unforced case. The strong recirculation persists and little of the river discharge has been dispersed by day 20. These winds drive northward flow at depth that brings water up the axis of the Hudson shelf valley.

Under westward wind the shape of the bulge becomes elongated and distorted because of surface horizontal shear resulting from the competition of geostrophic and Ekman flow. On the easternmost flank of the bulge Ekman flow tends to predominate and carry water northward, whereas closer to the center the buoyancy gradient is stronger and southward geostrophic flow prevails. There is a subsurface maximum in the southward flow, and the magnitude of the southward transport is second only to the southward wind case.

An analysis of momentum terms in the high-discharge scenarios shows that geostrophy and Ekman dynamics explain the force balance in almost all cases. The instances where the Rossby number is large enough to indicate a partial role of nonlinear momentum advection are in the case of the unforced plume, where Ro is 0.3 on the eastern side of the bulge; during westward winds where Ro is 0.25 in the constriction of flow, where the southern side of the bulge meets the

coastal current; and during southward winds within the coastal current itself south of the bulge, where Ro reaches 0.15 because of the magnitude ($v > 60$ cm s^{-1}) of the coastal jet.

The results described here that are of the greatest relevance to the objectives of the LaTTE program relate to the residence time within the apex of the New York Bight of waters discharged by the Hudson River during a typical spring freshet. During either northward or westward, and especially southward, winds the volume of freshwater stored in the apex of the bight begins to disperse about 1 week after the river discharge peaks. Without winds, or with eastward winds, the volume of freshwater residing close to the estuary mouth is still increasing for 10 days after the river flow peaks. For biogeochemical processes acting on time scales from several days to a week, this protracted residence time within the bight suggests that determining the fate of material transported by the Hudson River to the inner shelf will depend on transformation processes occurring within the apex of the New York Bight.

Acknowledgments. This study was supported by National Science Foundation Grants OCE-0238957 and OCE-0121506 and an IMCS Post-doctoral Fellowship to B.-J. Choi. High-performance computing resources were provided by the National Center for Atmospheric Research, which is funded by NSF. ROMS model development is supported by the Office of Naval Research. We thank H. Arango and G. Foti for assistance with the model configuration and R. Chant, R. Houghton, and S. Glenn for helpful discussions throughout the project.

REFERENCES

Beardsley, R. C., and W. C. Boicourt, 1981: On estuarine and continental shelf circulation in the Middle Atlantic Bight. *Evolution of Physical Oceanography,* B. A. Warren and C. Wunsch, Eds., MIT Press, 198–223.

——, ——, and D. V. Hansen, 1976: Physical oceanography of the Middle Atlantic Bight. *Limnol. Oceanogr. Special Symp.,* **2,** 20–34.

Blumberg, A. F., L. A. Khan, and J. P. St. John, 1999: Three-dimensional hydrodynamic model of New York Harbor region. *J. Hydraul. Eng.,* **125,** 799–816.

Bowman, M. J., 1978: Spreading and mixing of the Hudson River effluent into the New York Bight. *Hydrodynamics of Estuaries and Fjords,* J. C. J. Nihoul, Ed., Elsevier, 373–386.

——, and R. L. Iverson, 1978: Estuarine and plume fronts. *Oceanic Fronts in Coastal Processes,* M. J. Bowman and W. E. Esaias, Eds., Springer-Verlag, 87–104.

Chant, R. J., S. Glenn, E. Hunter, J. Kohut, R. F. Chen, and J. Wilkin, 2006: Bulge formation and cross-shelf transport of the Hudson estuarine discharge. *Eos, Trans. Amer. Geophys. Union,* **87** (Ocean Science Meeting Suppl.), Abstract OS34I-01.

Chao, S.-Y., and W. C. Boicourt, 1986: Onset of estuarine plumes. *J. Phys. Oceanogr.,* **16,** 2137–2149.

Fairall, C. W., E. F. Bradley, D. P. Rogers, J. B. Edson, and G. S. Young, 1996: Bulk parameterization of air-sea fluxes for Tropical Ocean-Global Atmosphere Coupled-Ocean Atmosphere Response Experiment. *J. Geophys. Res.,* **101,** 3747–3764.

——, ——, J. E. Hare, A. A. Grachev, and J. B. Edson, 2003: Bulk parameterization of air–sea fluxes: Updates and verification for the COARE algorithm. *J. Climate,* **16,** 571–591.

Fong, D. A., and W. R. Geyer, 2001: Response of a river plume during an upwelling favorable wind event. *J. Geophys. Res.,* **106,** 1067–1084.

——, and ——, 2002: The alongshore transport of freshwater in a surface-trapped river plume. *J. Phys. Oceanogr.,* **32,** 957–972.

García Berdeal, I., B. M. Hickey, and M. Kawase, 2002: Influence of wind stress and ambient flow on a high discharge river plume. *J. Geophys. Res.,* **107,** 3130, doi:10.1029/2001JC000932.

Harris, C. K., B. Butman, and P. Traykovski, 2003: Winter-time circulation and sediment transport in the Hudson shelf valley. *Cont. Shelf Res.,* **23,** 801–820.

Hetland, R. D., 2005: Relating river plume structure to vertical mixing. *J. Phys. Oceanogr.,* **35,** 1667–1688.

Hunter, E., R. J. Chant, J. Kohut, L. Bowers, and S. Glenn, 2006: Sea breeze forcing on the New Jersey shelf. *Eos, Trans. Amer. Geophys. Union,* **87** (Ocean Science Meeting Suppl.), Abstract OS35J-01.

Janzen, C. D., and K.-C. Wong, 2002: Wind-forced dynamics at the estuary-shelf interface of a large coastal plain estuary. *J. Geophys. Res.,* **107,** 3138, doi:10.1029/2001JC000959.

Johnson, D. R., J. Miller, and O. Schofield, 2003: Dynamics and optics of the Hudson River outflow plume. *J. Geophys. Res.,* **108,** 3323, doi:10.1029/2002JC001485.

MacCready, P., and W. R. Geyer, 2001: Estuarine salt flux through an isohaline surface. *J. Geophys. Res.,* **106,** 11 629–11 637.

Mellor, G. L., and T. Yamada, 1982: Development of a turbulence closure model for geophysical fluid problems. *Rev. Geophys. Space Phys.,* **20,** 851–875.

Mukai, A. Y., J. J. Westerink, R. A. Luettich, and D. J. Mark, 2002: Eastcoast 2001, a tidal constituent database for the western North Atlantic, Gulf of Mexico and Caribbean Sea. Engineer Research and Development Center/Coastal and Hydraulics Laboratory Tech. Rep. TR-02-24, 196 pp.

Peters, H., 1999: Spatial and temporal variability of turbulent mixing in an estuary. *J. Mar. Res.,* **57,** 805–845.

Pullen, J. D., and J. S. Allen, 2000: Modeling studies of the coastal circulation off northern California: Shelf response to a major Eel River flood event. *Cont. Shelf Res.,* **20,** 2213–2238.

Sanders, T. M., and R. W. Garvine, 2001: Fresh water delivery to the continental shelf and subsequent mixing: An observational study. *J. Geophys. Res.,* **106,** 27 087–27 101.

Shchepetkin, A. F., and J. C. McWilliams, 2005: The Regional Oceanic Modeling System (ROMS): A split-explicit, free-surface, topography-following-coordinate oceanic model. *Ocean Modell.,* **9,** 347–404.

Warner, J. C., W. R. Geyer, and J. A. Lerczak, 2005a: Numerical

modeling of an estuary: A comprehensive skill assessment. *J. Geophys. Res.,* **110,** C05001, doi:10.1029/2004JC002691.

——, C. R. Sherwood, H. G. Arango, R. P. Signell, and B. Butman, 2005b: Performance of four turbulence closure models implemented using a generic length scale method. *Ocean Modell.,* **8,** 81–113.

Whitney, M. M., and R. W. Garvine, 2005: Wind influence on a coastal buoyant outflow. *J. Geophys. Res.,* **110,** C03014, doi:10.1029/2003JC002261.

——, and ——, 2006: Simulating the Delaware Bay buoyant outflow: Comparison with observations. *J. Phys. Oceanogr.,* **36,** 3–21.

Wilkin, J. L., 2006: The summertime heat budget and circulation of southeast New England shelf waters. *J. Phys. Oceanogr.,* **36,** 1997–2011.

——, and L. Lanerolle, 2005: Ocean forecast and analysis models for coastal observatories. *Ocean Weather Forecasting: An Integrated View of Oceanography,* E. P. Chassignet and J. Verron, Eds., Springer, 549–572.

Yankovsky, A. E., and D. C. Chapman, 1997: A simple theory for the fate of buoyant coastal discharges. *J. Phys. Oceanogr.,* **27,** 1386–1401.

——, B. M. Hickey, and A. Münchow, 2001: Impact of variable inflow on the dynamics of a coastal plume. *J. Geophys. Res.,* **106,** 19 809–19 824.